Elementary excitations, exchange interaction and spin-Peierls transition in CuGeO3

Khomskii, D.I; Geertsma, W.; Mostovoy, M.V.

Published in:
Czechoslovak Journal of Physics

DOI:
10.1007/BF02548136

Publication date:
1996

Proceedings of the 21st International Conference on Low Temperature Physics
Prague, August 8-14, 1996

Part S6 - Plenary and invited papers

Elementary excitations, exchange interaction and spin-Peierls transition in $CuGeO_3$

D. Khomskii[a,b], W. Geertsma[a], and M. Mostovoy[a,c]

[a] Groningen University,
Nijenborgh 4, 9747 AG Groningen, the Netherlands

[b] P. N. Lebedev Physical Institute,
Leninski prosp.53, Moscow, Russia

[c] G. I. Budker Institute of Nuclear Physics,
630090 Novosibirsk, Russia

The microscopic description of the spin-Peierls transition in pure and doped $CuGeO_3$ is developed taking into account realistic details of crystal structure. It it shown that the presence of side-groups (here Ge) strongly influences superexchange along Cu–O–Cu path, making it antiferromagnetic. Nearest-neighbour and next-nearest neighbour exchange constants J_{nn} and J_{nnn} are calculated. Si doping effectively segments the CuO_2-chains leading to $J_{nn}(\mathrm{Si}) \simeq 0$ or even slightly ferromagnetic. Strong sensitivity of the exchange constants to Cu–O–Cu and (Cu–O–Cu)–Ge angles may be responsible for the spin-Peierls transition itself ("bond-bending mechanism" of the transition). The nature of excitations in the isolated and coupled spin-Peierls chains is studied and it is shown that topological excitations (solitons) play crucial role. Such solitons appear in particular in doped systems ($Cu_{1-x}Zn_xGeO_3$, $CuGe_{1-x}Si_xO_3$) which can explain the $T_{SP}(x)$ phase diagram.

1. Introduction

The low-dimensional materials are known to be very susceptible to various instabilities, such as formation of charge- or spin-density waves. Probably, the first one discussed is the famous Peierls instability of one-dimensional metals: lattice distortion with the new lattice period $2\pi/Q$, where the wave vector $Q = 2k_F$ (if there is one electron per site, the lattice dimerizes). The lattice distortion opens a gap in the electron spectrum at the Fermi surface, so that the energies of all occupied electron states decrease, which drives the transition. It is also known that this instability survives when we include the strong on-site Coulomb repulsion between electrons (the, so called, Peierls-Hubbard model),

$$H = -\sum_{l,\sigma}(J_0 + \alpha(u_l - u_{l+1}))\left(c^\dagger_{l\sigma}c_{l+1\sigma} + h.c.\right) + U\sum_l c^\dagger_{l\uparrow}c_{l\uparrow}c^\dagger_{l\downarrow}c_{l\downarrow} + \sum_l\left(\frac{P_l^2}{2M} + \frac{K}{2}(u_{l+1}-u_l)^2\right) \quad (1)$$

Here the first term describes the dependence of the electron hopping integral $t_{l,l+1}$ on the change of the distance $u_l - u_{l+1}$ between the neighbouring ions and the last term is the lattice energy (which after quantization becomes $\sum_q \omega_q b^\dagger_q b_q$). The dimensionless electron–lattice coupling constant $\lambda = 4\alpha^2/(\pi t_0 K)$ determines the magnitude of the lattice distortion and the energy gap.

When Coulomb repulsion is strong, $U \gg t_0$, and there is one electron per site, we are in the limit of localized electrons (Mott-Hubbard insulator) with effective antiferromagnetic interaction (Spin-Peierls model),

$$H_{eff} = \sum_l J_{l,l+1}\,\mathbf{S}_l \cdot \mathbf{S}_{l+1} + \sum_l\left(\frac{P_l^2}{2M} + \frac{K}{2}(u_{l+1}-u_l)^2\right), \quad (2)$$

where the exchange constant $J_{l,l+1} = J_0 + \alpha'(u_l - u_{l+1})$, $J_0 = 4t_0^2/U$ and $\alpha' = 8t_0\alpha/U$. The dependence of $J_{l,l+1}$ on the distance between neighbouring spins again leads to an instability, as the result of which the spin chain dimerizes. Physically it corresponds to a formation of singlet dimers—the simplest configuration in the valence bond picture. This

transition, known as the spin-Peierls (SP) transition, was extensively studied theoretically [1, 2, 3] and was previously observed experimentally in a number of quasi-one-dimensional organic compounds, such as TTF-CuBDT ($T_{SP} = 12K$) or TTF- AuBDT ($T_{SP} = 2.1K$) [4].

Recently the first inorganic spin-Peierls material $CuGeO_3$ was discovered [5]. Since then much experimental data on this material, both pure and doped (mostly by Zn and Si), was obtained. The spin chains in this compound are formed by CuO_4 plaquettes with common edge (See Fig.1). They apparently play the main role in the spin-Peierls transition with $T_{SP} = 14K$. However, as we will discuss below, the interchain interaction is also very important here. The interchain coupling is provided both by Ge ions (along b-axis of the crystal) and by the well separated apex oxygens (along a-axis; direction of the chains coincides with the c-axis of a crystal).

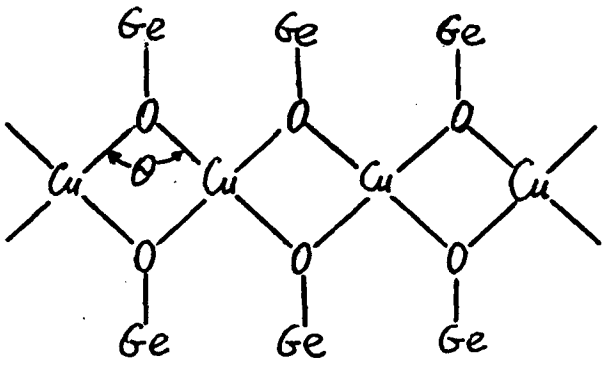

FIG. 1. Simplified structure of CuO_2 chains in $CuGeO_3$.

Experimentally it is established that the strongest anomalies in $CuGeO_3$, both in the normal phase and at the spin-Peierls transition, occur not along the c-axis, but, rather unexpectedly, along the other two directions, the strongest one found along the b-axis [6, 7]. For instance, the anomalies in the thermal expansion coefficient and in the magnetostriction along the b-axis are several times stronger than along the direction of the chains [7, 8].

Further interesting information is obtained in the studies of doping dependence of various properties of $CuGeO_3$. It was shown that the substitution of Cu by nonmagnetic Zn, as well as Ge by Si, leads initially to a rather strong reduction of T_{SP} [9, 10], which according to some recent data [11] is flattened out at higher doping level. Simultaneously, antiferromagnetic order develops at lower temperatures, often coexisting with the SP distortion [11, 12].

The aim of the present investigation is to provide microscopic picture of the properties of $CuGeO_3$ taking into account realistic details of its structure. We will address below several important issues:

- The detailed description of the exchange interaction (Why is nearest neighbour exchange antiferromagnetic?);
- The sensitivity of the exchange constants to different types of distortion and the resulting from that microscopic picture of the spin-Peierls transition, which may be called bond-bending model (Why the anomalies are strongest in the perpendicular directions? Why is SP transition observed in $CuGeO_3$ and not in many other known quasi-one-dimensional magnets?);
- The nature of elementary excitations in spin-Peierls systems in general (Are they the ordinary singlet-triplet excitations? How are they influenced by the interchain interaction?);
- The mechanism by which doping affects the properties of SP system (Why is the effect so strong? Why does the system develops antiferromagnetic order upon doping?).

These questions are raised by the experimental observations, and we hope that their clarification will help both to elucidate some general features of SP transitions and to build the detailed picture of this transition in $CuGeO_3$.

2. Exchange Interaction in $CuGeO_3$. Role of Side-Groups in Superexchange

The first question we would like to address is: why is the nearest-neighbour Cu-Cu exchange interaction antiferromagnetic at all? The well-known Goodenough-Kanamori-Anderson rules state, in particular, that the 90°-exchange between two half-filled orbitals is ferromagnetic. In $CuGeO_3$ the Cu-O-Cu angle θ in the superexchange path is 98°, which is rather close to 90°. Usually, the antiferromagnetic character of the exchange is attributed to this small 8° difference. Our calculation [13], however, shows that it is not enough: even in this realistic geometry the exchange constant for the nearest neighbour (nn) spins for realistic values of parameters (such as copper-oxygen overlap, magnitude of the Coulomb

interaction on copper and oxygen, Hund's rule intraatomic exchange, etc) is still slightly ferromagnetic, $J^c_{nn} = -0.6$meV.

To explain the observed values of J^c_{nn} the idea was put forward in [13] that the antiferromagnetic coupling may be enhanced by the, initially ignored, side-groups effect (here Ge). As it is clear from Fig.1, there is a Ge ion attached to each oxygen in CuO_2 chain. The Coulomb interaction with Ge^{4+} and the hybridization of $2p_y$ orbital of oxygen with Ge (see Fig.2) destroys the equivalence of p_x-orbitals (shaded) and p_y-orbitals (empty) of oxygen, which for 90°-exchange was responsible for the cancellation of the corresponding antiferromagnetic contributions to superexchange. As a result, the exchange with partial delocalization into Ge may become antiferromagnetic even for 90° geometry (for a detailed discussion see [13]). The calculation gives a reasonable value for the nearest-neighbour exchange interaction: $J^c_{nn} = 11.6$meV (the experimental value is $9 \div 15$meV, depending on the procedure of extraction of J^c_{nn} from the experimental data).

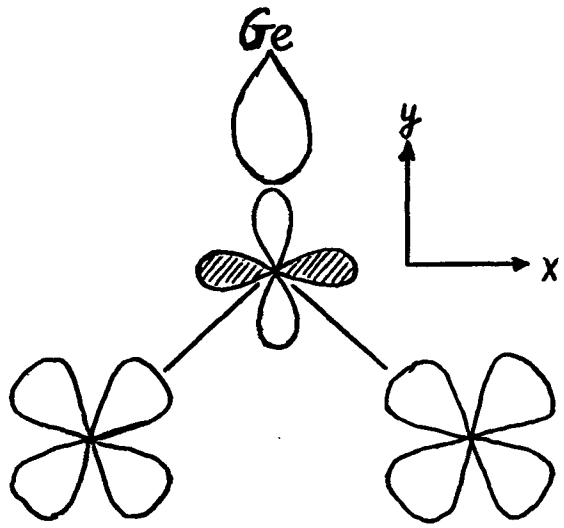

FIG. 2. Electronic orbitals relevant for superexchange.

We also calculated other exchange constants using a similar approach. For the interchain interaction along b and a axes we obtained $J^b_{nn} = 0.7$meV and $J^a_{nn} = -3 \cdot 10^{-4}$meV, so that $J^b_{nn}/J^c_{nn} \approx 0.06$, and $J^a_{nn}/J^c_{nn} \approx -3 \cdot 10^{-5}$. The experimental values are: $J^b_{nn}/J^c_{nn} \approx 0.1$, $J^a_{nn}/J^c_{nn} \approx -0.01$. Thus our theoretical results are not so far from the experiment for the interchain interaction in the b-direction and too small for a-axis. We note, however, that the ferromagnetic exchange in a-direction is in any event very weak and a small variation of parameters used in our calculation can easily changes this value quite significantly.

More interesting is the situation with the next-nearest-neighbour (nnn) interaction in the chain direction J^c_{nnn}. As is clear from Figs.1 and 2, there is a relatively large overlap of the p_x orbitals on neighbouring plaquettes, which leads to a rather strong antiferromagnetic nnn coupling. Our calculation gives $\gamma = J^c_{nnn}/J^c_{nn} \approx 0.23 \div 0.3$. From the fit of $\chi(T)$ curve Castilla *et al* [14] obtained the value $\gamma \approx 0.25$. Note also that a sufficiently strong nnn interaction may lead to a singlet formation and creation of a spin gap even without the spin-lattice interaction. Such a state is an exact ground state at the Majumdar-Ghosh point $\gamma = 0.5$ [16]. The critical value for appearance of a spin gap is $\gamma \approx 0.25$ [14]. Thus, from both the fit to experimental data and our calculations it appears that $CuGeO_3$ is rather close to the critical point, so that one can conclude that both the frustrating nnn interaction and the spin-lattice interaction combine to explain the observed properties of $CuGeO_3$ (see also [8]).

Anticipating the discussion below, we consider here the modification of the exchange constants caused by doping. In particular, we calculated the change of J^c_{nn} when Ge ion attached to a bridging oxygen is substituted by Si. As Si is smaller than Ge, one can expect two consequences. First, it will pull closer the nearby chain oxygen, somewhat reducing the corresponding Cu-O-Cu angle θ. The second effect is the reduced hybridization of $2p_y$ orbital of this oxygen with Si. According to the above considerations (see also [13]) both these factors would diminish the antiferromagnetic nn exchange. Our calculation shows [16] that for realistic values of parameters the resulting exchange interaction becomes either very small or even weakly ferromagnetic, $J^c_{nn} = 0 \pm 1$meV. Thus Si doping effectively interrupts the chains similar the effect of substituting Cu by Zn. This result will be used later in section 5.

3. Bond-Bending Model of the Spin-Peierls Transition in $CuGeO_3$

We return to the discussion of the exchange interaction and its dependence on the details of crystal structure of $CuGeO_3$. As follows from the previous section, the largest exchange constant J^c_{nn} is very sensitive to both Cu-O-Cu angle θ and to the side group (here Ge). As to the second factor, one has to

take into account that, contrary to a simple model of $CuGeO_3$ shown in Fig.2, in the real crystal structure Ge ion lies not exactly in the plane of CuO_2 chain: the angle α between Ge and this plane is $\sim 160°$. The actual crystal structure may be schematically depicted as in Fig.3, where the dashed lines represent CuO_2-chains.

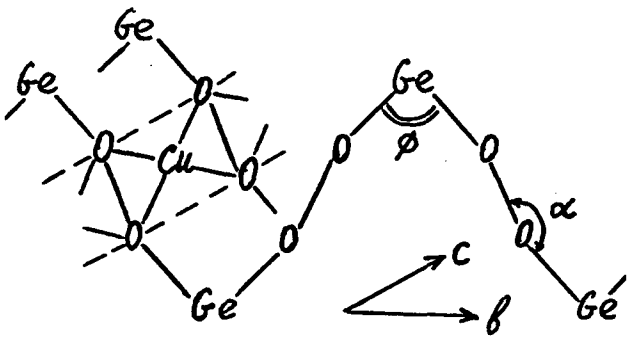

FIG. 3. Schematic structure of CuO_2 - Ge skeleton in $CuGeO_3$.

One can easily understand that J^c_{nn} is also very sensitive to a Ge-CuO_2 angle α. The influence of Ge, which according to the above consideration gives an antiferromagnetic tendency, is the largest when $\alpha = 180°$: just in this case the inequivalence of $2p_x$ and $2p_y$ orbitals shown in Fig.2, which is crucial for this effect, becomes the strongest. On the other hand, if, for instance, $\alpha = 90°$ (*i.e.* if Ge would sit exactly above the oxygen) its interaction with $2p_x$ and $2p_y$ orbitals would be the same and the whole effect of Ge on J^c_{nn} would disappear. Thus bending GeO-bonds with respect to CuO_2-plane would change J^c_{nn} (it becomes smaller when α decreases).

These simple considerations immediately allows one to understand many, at first glance, strange properties of $CuGeO_3$ mentioned in the introduction [18]. Thus, *e.g.* the compression of $CuGeO_3$ along the *b*-direction would occur predominantly by way of decreasing of Ge-(CuO_2) angle α, while the tethrahedral O-Ge-O angle ϕ is known to be quite rigid. Such a "hinge" or "scharnier" model explains why the main lattice anomalies are observed along the *b*-axis [7] and why the longitudinal mode parallel to *b* is especially soft [6]. Within this model one can also naturally explain (even quantitatively) the fact that the magnetostriction is also strongest in the b-direction [8]. If we assume that the main changes in the lattice parameters occur only due to bond bending (*i.e.* due to the change of angles, while bond lengths remain fixed), we obtain the following result for the uniaxial pressure dependence of $J \equiv J^c_{nn}$ [18]: $\delta J/\delta P_b = -1.5\text{meV/GPa}$, which is close to the experimental result $\delta J/\delta P_b = -1.7\text{meV/GPa}$ [8]. We can also explain reasonably well the change of the exchange coupling for other directions.

This picture can be also used to explain the spin-Peierls transition itself. What occurs below T_{SP}, is mostly the change of bond angles ("bond-bending"), which alternates along the chains. Experimentally it was found [19] that the dimerization is accompanied by the alternation of Cu-O-Cu angles θ. In our model J is also sensitive to Ge-CuO_2) angle α and we speculated in Ref.14 that this angle, most probably, also alternates in the spin-Peierls phase. Recently this alternation was observed [17].

Consequently we have a rather coherent picture of the microscopic changes in $CuGeO_3$, both above and below T_{SP}: in the first approximation we may describe the main lattice changes as occurring mostly due to the change of the "soft" bond angles. The strongest effects for $T > T_{SP}$ are then expected along the *b*-axis, which is consistent with the experiment. The same bond-bending distortions seem also to be responsible for the spin-Peierls transition itself, the difference with the normal phase being the alternation of the corresponding angles in the *c*-direction.

The bond-bending model allows one to explain another puzzle related to spin-Peierls transitions (discussed already in [2]): up to now such transitions have been observed only in a few of the many known quasi-one-dimensional antiferromagnets. There might be several reasons for that. The first one is that the spin-Peierls phase in $CuGeO_3$ is, at least partially, stabilized by the frustrating next-nearest neighbour interaction J^c_{nnn}. The other factor is that the spin-Peierls instability is greatly enhanced when the corresponding phonon mode is soft enough [2]. One can see it *e.g.* from the expression for T_{SP} [3],

$$T_{SP} = 0.8\lambda' J \ .$$

The spin-phonon coupling constant is

$$\lambda' = \frac{\alpha'^2}{JK} = \frac{\alpha'^2}{JM\omega_0^2} \ ,$$

where $\omega_0 = \sqrt{K/M}$ is the typical phonon frequency.

There is, usually, a competition between the $3d$ magnetic ordering and the spin-Peierls phase. Apparently, in most quasi-one-dimensional compounds the $3d$ magnetic ordering wins, and for the spin-Peierls transition to be realized a strong spin-lattice

coupling,*i.e.* rather soft phonons, is necessary. Such soft phonon modes are known to exist in the organic spin-Peierls compounds [2]. In $CuGeO_3$ it can be rather soft bond-bending phonons, especially the ones parallel to the b-axis, which help to stabilize the spin-Peierls phase relative to the $3d$ antiferromagnetic one. Nevertheless, a relatively small doping is sufficient to make the antiferromagnetic state more favourable, although some other factors are also very important here, as will become clear in the next section.

4. Solitons and Strings in Spin-Peierls Systems

Let us turn now to the second group of problems related to SP systems, namely, the nature of elementary excitations. In the simple picture mentioned in the introduction (and valid in the strong coupling limit) the SP state consists of isolated dimers. For the rigid dimerized lattice an excited state is a triplet localized on one of the dimers and separated from the ground state by an energy gap J. The interaction between the neighbouring dimers gives a certain dispersion to this excitation, transforming it into an object similar to a usual magnon.

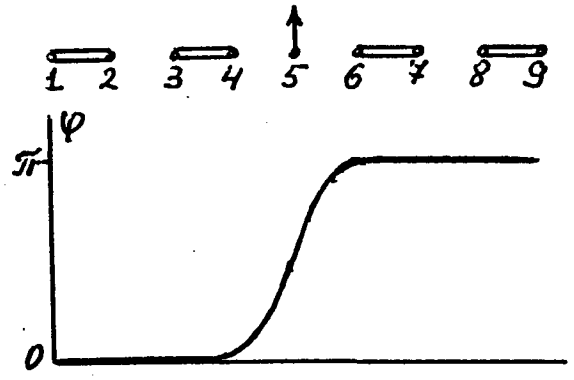

FIG. 4. SP soliton in the strong coupling limit (above) and in the continuum model (below).

If, however, the lattice is allowed to adjust to a spin flip, the localized triplet decays into a pair of topological excitations. Such excitations (solitons or kinks) are known to be the lowest energy excitations in electronic Peierls insulators [20]. The same is also true for spin-Peierls systems. Indeed, there exist two degenerate ground states in a SP chain: one with singlets formed on sites ...(12)(34)(56)..., and another of the type ...(23)(45)(67).... One can characterize them by the phase of the order parameter ϕ_n, so that $\phi_n = 0$ in the first state and $\phi_n = \pi$ in the second. The soliton is an excited state, in which the order parameter interpolates from 0 to π or vice versa. In the strong coupling limit such a state looks like ...(12)(34)↑(67)(89)..., see Fig. 4. Actually, the soliton has a finite width, which (as the correlation length in the BCS theory) has a form,

$$\xi_0 \left(= \frac{\hbar v_F}{\Delta_0}\right) \sim \frac{J}{\Delta} a \sim \frac{J}{E_s} a \ . \qquad (3)$$

Here the Fermi velocity $v_F \sim Ja/\hbar$ is the velocity of the spinless Jordan-Wigner fermions, in terms of which the Hamiltonian (2) has a form similar to the Hamiltonian of the electronic Peierls system, 2Δ is the energy gap and a is the lattice constant, which below we will put equal to 1. The excitation energy of the SP soliton, E_s, can easily be determined for the XY-model, *i.e.* if one ignores $S_l^z \cdot S_{l+1}^z$ term in the Hamiltonian (2). Then the spin-Peierls Hamiltonian (2) after the Jordan-Wigner transformation acquires a form of the Su-Schrieffer-Heeger Hamiltonian [20] for electronic Peierls materials, in which case $E_s = \frac{2}{\pi}\Delta$ [20]. The omitted term renormalizes the soliton energy, as well as the mean-field energy gap 2Δ, but these numerical changes do not play an important role. One should also note that the kinks are mobile excitations with the dispersion $\sim E_s$. In $CuGeO_3$ ξ_0 is estimated to be of the order of 8 lattice spacings.

From Fig.4 it is clear that a soliton in SP system corresponds to one unpaired spin. Thus, these elementary excitations have $\frac{1}{2}$ rather then 1 as the singlet-triplet excitations. Of course, for fixed boundary conditions the solitons (excited *e.g.* thermally or optically) always appear in pairs.

So far we considered the excitations in an isolated SP chain. Now we want to include the effects of the interchain interaction. Due to this interaction (mediated, for instance, by three-dimensional phonons) SP distortions of neighbouring chains would prefer to be phase coherent, *e.g.* in phase. When a kink-antikink pair of size r is created in one of the chains, the phase of the distortion between the kink and antikink is opposite to the initial one as well as to those on neighbouring chains, which would cost an energy $E(r) = Z\sigma r$, where σ is the effective interaction between the Peierls phases on different chains per one link and Z is the number of neighbouring chains (See Fig.5a). Therefore, in the presence of the interchain interaction the soliton-antisoliton pair forms a string and $Z\sigma$ may be called the string tension. The linear potential of the string confines the soliton motion, *i.e.* kink and antikink can not go far from each other

in an ordered phase.

We can use this picture to estimate the value of the temperature of the $3d$ SP transition. The concentration of thermally excited kinks in an isolated chain is $n = \exp(-E_s/T)$ and the average distance between them is $\bar{d}(T) = n^{-1} = \exp(E_s/T)$. At the same time, the average distance between the kinks connected by string is $\bar{l}(T) = T/(Z\sigma)$. The three-dimensional phase transition (ordering of phases of the lattice distortions of different chains) occurs when $\bar{l}(T) \sim \bar{d}(T)$, *i.e.*

$$\frac{T_{SP}}{Z\sigma} \sim \exp\left(\frac{E_s}{T_{SP}}\right) , \tag{4}$$

or

$$T_{SP} \sim \frac{E_s}{\ln \frac{E_s}{Z\sigma}} \sim \frac{\lambda' J}{\ln\left(\frac{\lambda' J}{Z\sigma}\right)} \tag{5}$$

where we use the relation $E_s \sim \Delta \sim \lambda' J$ [3]. In this picture at $T < T_{SP}$ the phases of SP distortions of different chains are correlated and all solitons are paired. At $T > T_{SP}$ local SP distortions still exist in each chain, but there is no long range order. Therefore, the SP transition in this picture is of a "deconfinement" type, which is somewhat similar to the Kosterlitz-Thouless transition in $2d$-systems.

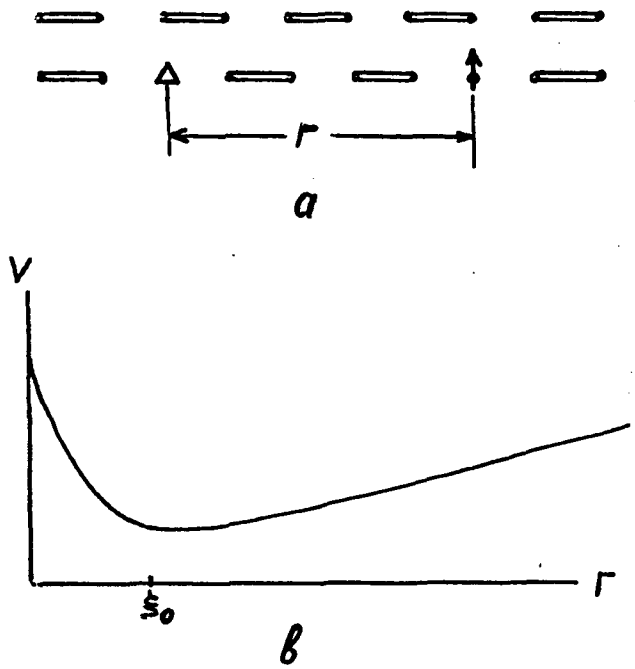

FIG. 5. (a) A string confining a soliton to an impurity (indicated by a triangle); (b) total potential acting on the soliton near the impurity.

The approach described above is valid when the value of the interchain interaction σ is much smaller than J. Using Eq.(5) with $J = 100$K and $\lambda' \sim 0.2$ [5] we get $\sigma \sim 0.04J$, which in view of the logarithmic dependence of T_{SP} on σ in (5) is just enough for applicability of the results presented above (these are, of course, only an order of magnitude estimates).

5. Solitons in Doped Systems

As we have seen above, Zn and Si, the two most studied dopands of $CuGeO_3$, lead to an effective interruption of spin chains into segments of finite length. The segments with even number of Cu ions can have a perfect SP ordering, while the odd segments behave differently: one spin $\frac{1}{2}$ remains unpaired, which means that the ground state of an odd segment contains a soliton (similarly to what happens in the electronic Peierls materials [21]). One can show that the soliton is repeled by ends of the segment, and in an isolated odd segment the situation would look like in Fig.4: the soliton carrying spin $\frac{1}{2}$ would prefer to stay in the middle of a segment. This conclusion is in contrast with the usual assumption that the magnetic moments induced by doping are localized near the impurities.

The situation, however, changes when we take into account the interchain interaction. As we have seen in the previous section, moving a soliton along a chain costs an energy which grows lineary with the distance. As is illustrated in Fig.5a, this provides a force pulling the soliton back to the impurity. Thus the soliton moves in a potential shown in Fig.5b: it repels from the impurity with the potential $V_{imp}(r) \sim J\exp(-r/\xi_0)$, while the interchain interaction gives the potential $V_{conf}(r) \sim Z\sigma r$, providing the restoring force. As a result, the soliton is located at a distance $\sim \xi_0$ from impurity, so that, in a sense, we return to the traditional picture. One should keep in mind, however, that for a weak interchain interaction the total potential $V_{imp} + V_{conf}$ is rather shallow and at finite temperature the soliton can go rather far from impurity. It seems that it should be possible to check this picture experimentally, *e.g.* by detailed NMR study of doped SP compounds (cf. the results of M. Chiba *et al*, this conference).

6. Phase Diagram of Doped Spin-Peierls Systems

One can use this picture to describe qualitatively the dependence of the phase transition temperature T_{SP} on the concentration of dopands x. Similar to the treatment given in section 4, we compare an average distance between the kink and the nearest end of

the segment $\bar{l}(T) \sim T/(Z\sigma)$ with the average length of the segment $\bar{d} \sim 1/x$. This gives,

$$T_{SP}(x) \sim \frac{Z\sigma}{x} \ . \qquad (6)$$

This result has two limitations. At large x, when an average length of the segment becomes of the order of soliton size, $1/x \sim \xi_0$, there will be no ordering even at $T = 0$. Thus $x \sim \xi_0^{-1}$ is an absolute limit beyond which the $3d$ ordering disappears. Using our estimate $\xi_0 \sim 8$, such $x_{max} \sim 15\%$. On the other hand, the result (6) is also not valid at very small x. When an average size of segment $\bar{d}(x) \sim 1/x$ becomes sufficiently large, the thermally induced solitons become as important as the solitons induced by disorder. In this case the total concentration of solitons is

$$n_{tot} = n_{imp} + n_{therm} = x + e^{-\frac{E_s}{T}} \ , \qquad (7)$$

and one should compare $\bar{l}(T)$ with n_{tot}^{-1}. For $x = 0$ we return to Eq.(5), while for small x we get,

$$T_{SP}(x) = T_{SP}(0)(1 - \alpha x) \ , \qquad (8)$$

where the coefficient α is

$$\alpha \sim \frac{E_s}{Z\sigma \ln\left(\frac{E_s}{Z\sigma}\right)} . \qquad (9)$$

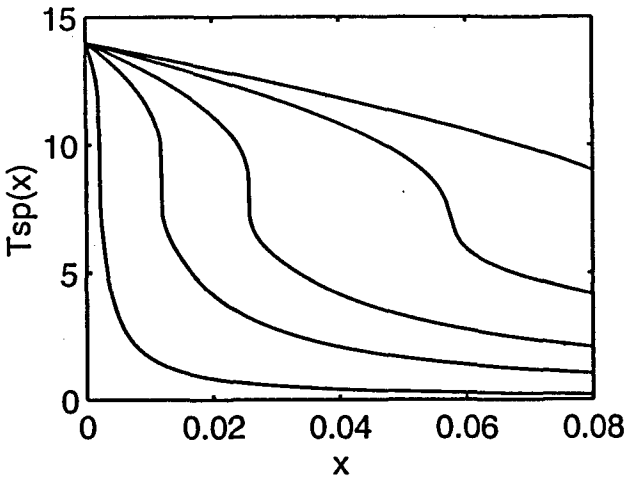

FIG. 6. Dependence of the SP transition temperature on the concentration of dopands for several values of interchain coupling.

One can verify these estimates more rigorously by mapping the spin-Peierls system onto an effective Ising model. Let us associate the classical Ising variable $\tau = \pm 1$ with the two possible types of SP ordering (phases 0 and π), so that the phase 0 (left domain in Fig.4) corresponds to $\tau = +1$, while the phase π (right domain in the same figure) corresponds to $\tau = -1$. In this language a soliton is a domain wall in Ising variables. Since it costs an energy E_s to create a soliton, the Hamiltonian of the intrachain interaction in the effective Ising model can be written as,

$$H_{intra} = -\frac{E_s}{2} \sum_{n,\alpha} (\tau_{n,\alpha}\tau_{n+1,\alpha} - 1) \ , \qquad (10)$$

(here α is the chain index and n is the site number in chain). Similarly, an interchain interaction in terms of Ising variables has a form,

$$H_{inter} = -\frac{\sigma}{2} \sum_{n,\alpha} \tau_{n,\alpha} \sum_{\delta} \tau_{n,\alpha+\delta} \ , \qquad (11)$$

where the summation over δ goes over neighbouring chains. One can also introduce impurities in this effective Ising model. The detailed treatment of this model will be given in a separate publication [22]. Here we limit ourselves by presenting in Fig.6 the results of the numerical solution of the equation for the transition temperature for several values of the interchain interaction σ. The value of J was adjusted to make the transition temperature equal to 14K for each value of σ. The values of σ (from the top curve to the bottom one) are (in K) 3; 2; 1; 0.5; 0.1. We see that the behaviour of $T_{SP}(x)$ agrees with the (6) at large x and (8) at small x and for the values of the parameter σ not much different from the estimates made in section 4 one can obtain a reasonable form of the phase diagram for $CuGeO_3$. (One should also take into account that each Ge is coupled to two chains, so that its substitution by Si introduces two interruptions in exchange interaction, whereas Zn interrupts only one chain.)

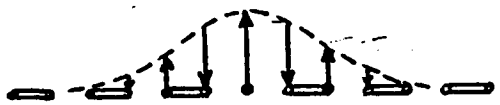

FIG. 7. Antiferromagnetic correlations around the soliton.

As follows from our picture, each soliton introduced by doping carries an uncompensated spin $\frac{1}{2}$.

One can easily show that in the vicinity of the domain wall where the SP order parameter is small there exist antiferromagnetic spin correlations (see Fig.7). Both these correlations and the SP distortion change on a length scale ξ_0. Antiferromagnetic correlations on neighbouring kinks may overlap, which could, in principle, lead to the long-range antiferromagnetic ordering. Thus it is possible to obtain a regime in which the SP and antiferromagnetic orderings coexist. To study this question in detail one must also take into account also the interchain exchange interaction. This question is now under investigation [24].

7. Concluding Remarks

To summarize we have a rather coherent picture of the main properties of the SP system $CuGeO_3$. The treatment given in the first part of this paper allows one to explain many of the features of this compound, which, at first glance, look rather puzzling, such as the strong anomalies observed in the direction perpendicular to chains rather than parallel to them. Furthermore we showed how the local geometry and the side-groups (Ge, Si) lead to a rather detailed microscopic picture of the distortions in $CuGeO_3$ both above and below T_{SP}. These results are largely specific for this particular compound, although some of the conclusions (*e.g.* the role of side groups in superexchange and the importance of the soft bending modes) are of a more general nature.

The results of the second part of the paper, though inspired by the experiments on $CuGeO_3$, have a general character, *e.g.* the conclusions about the domain wall structure of the elementary excitations, confinement of solitons caused by the interchain interaction, disorder-induced solitons [23], etc. At the same time, this general treatment provides a reasonable explanation of the suppression of T_{SP} by doping and allows to describe, at least qualitatively, the phase diagram of doped $CuGeO_3$.

We are grateful to J. Knoester, A. Lande, O. Sushkov and G. Sawatzky for useful comments. D. Kh. is especially grateful to B. Büchner for extremely useful discussions and for informing him of many experimental results prior to publication. This work was supported by the Dutch Foundation for Fundamental Studies of Matter (FOM).

REFERENCES

[1] E. Pytte, Phys. Rev. B **10**, 4637 (1974).

[2] L. N. Bulaevskii, A. I. Buzdin, and D. I. Khomskii, Solid State Commun. **27**, 5 (1978).

[3] M. C. Cross and D. S. Fisher, Phys. Rev. B **19**, 402 (1979); M. C. Cross, Phys. Rev. B **20**, 4606 (1979).

[4] J. W. Bray *et al*, in *"Extended Linear Chain Compounds"*, ed. J. S. Miller, (Plenum, NY 1985), p.353.

[5] M. Hase, I. Terasaki, and K. Uchinokura, Phys. Rev. Lett. **70**, 3651 (1993).

[6] J. E. Lorenzo *et al*, Phys. Rev. B **50**, 1278 (1994).

[7] H. Winkelmann *et al*, Phys. Rev. B **51**, 12884 (1995).

[8] B. Büchner *at al*, Phys. Rev. Lett. in press.

[9] M. Hase *et al*, Phys. Rev. Lett. **71**, 4059 (1993).

[10] J. P. Renard *et al*, Europhys. Lett. **30**, 475 (1995).

[11] Y. Sasago *et al*, preprint cond-mat/9603185.

[12] L. P. Regnault *et al*, Europhys. Lett. **32**, 579 (1995).

[13] W. Geertsma and D. Khomskii, Phys. Rev. B **54** (1996).

[14] G. Castilla, S. Chakravarty and V. J. Emery, Phys. Rev. Lett. **75**, 1823 (1995).

[15] C. K. Majumdar and D. K. Ghosh, J. Math. Phys. **10**, 1388, 1899 (1969).

[16] W. Geertsma and D. Khomskii, to be published.

[17] M. Braden *et al*, preprint 1996.

[18] B. Büchner, W. Geertsma and D. Khomskii, to be published.

[19] K. Hirota *et al*, Phys. Rev. Lett. **31**, 736 (1994).

[20] A. J. Heeger, S. Kivelson, J. R. Schrieffer, and W. P. Su, Rev. Mod. Phys. **60**, 781 (1988).

[21] W. P. Su, Solid State Commun. **35**, 899 (1980).

[22] M. Mostovoy and D. Khomskii, to be published.

[23] M. Mostovoy, M. T. Figge, and J. Knoester, to be published.

[24] The coexistence of the SP and the antiferromagnetic phases was recently treated by H. Fukuyama, T. Tanimoto and M. Saito, J. Phys. Soc. Japan, **65**, 1182 (1996). Our approach is rather similar, with one important difference: due to the presence of solitons the change of phase by π is allowed in our picture, whereas it is not realized in the solution obtained in the above cited paper.